

RINGO3 polarimetry of the Type I superluminous SN 2017egm

Justyn R. Maund¹,¹★† Iain Steele,² Helen Jermak,² J. Craig Wheeler³ and Klaas Wiersema⁴

¹Department of Physics and Astronomy, University of Sheffield, Hicks Building, Hounsfield Road, Sheffield S3 7RH, UK

²Astrophysics Research Institute, Liverpool John Moores University, IC2 Liverpool Science Park, 146 Brownlow Hill, Liverpool L3 5RF, UK

³Department of Astronomy, University of Texas at Austin, C1400 University Station, Austin, TX 78712, USA

⁴Department of Physics, University of Warwick, Coventry CV4 7AL, UK

Accepted 2018 October 27. Received 2018 October 23; in original form 2018 June 19

ABSTRACT

The origin of the luminosity of superluminous supernovae (SLSNe) is an unresolved mystery, and a number of very different physical scenarios (including energy injection from magnetars, collision with a dense circumstellar medium, and pair instability-induced explosions) have been invoked. The application of polarimetry to normal SNe has been shown to probe the three-dimensional structure of exploding stars, providing clues to the nature of the explosion mechanism. We report imaging linear polarimetry observations of the Type I SLSN 2017egm, in the galaxy NGC 3191, conducted with the Liverpool Telescope and the *RINGO3* instrument. Observations were acquired at four epochs, spanning 4–19 d after light curve maximum, however, polarization was not detected at a level of $>3\sigma$. At +7 and +15 d, and in the average over all epochs, we find a possible polarization signal, detected at a significance of $\approx 2\sigma$ in the ‘blue’ channel. This signal is seen, primarily, in the Stokes q parameter, with a corresponding polarization angle consistent with the orientation of the spiral arm in proximity to the position of SN 2017egm. We interpret this as indicating that any polarization, if present, originates from dust in the host galaxy rather than being intrinsic to the SN itself. Despite its apparent peculiarities, compared to other Type I SLSNe, the polarization characteristics of SN 2017egm are consistent with the previously reported low polarization of other SLSNe of this variety.

Key words: techniques: polarimetric – supernovae: general – supernovae: individual: 2017egm.

1 INTRODUCTION

With the discovery of the extremely bright supernovae (SNe) 2005ap (Quimby et al. 2007) and 2006gy (Smith et al. 2007), it was realized that there exists a distinct class of ‘superluminous’ (SL) SNe, whose extreme brightness breaks the paradigm of the energetic death of massive stars powered by the collapse of an iron core. Superluminous supernovae (SLSNe) constitute some of the brightest transients in astronomy, reaching absolute magnitudes of $M \sim -21$ mag (for a review see Gal-Yam 2012). The current record for the brightest transient is ASASSN-15lh, which has been interpreted as being a SLSN (Dong et al. 2016, however, for an alternative explanation see Leloudas et al. 2016). The origin of their luminosity still remains unclear with a number of different competing engines being invoked to explain the high luminosities, such as the decay of significant

quantities of radioactive nickel produced in pair-instability induced explosions (Gal-Yam et al. 2009), energy injection from the spin-down of a newly formed magnetar (Kasen & Bildsten 2010), and interaction with a dense circumstellar medium (see e.g. Woosley, Blinnikov & Heger 2007; Chatzopoulos & Wheeler 2012).

Controversially, the ‘smoking gun’ piece of observational evidence for the nature of the engine responsible is still absent. The bulk of observations of SLSNe are concerned with photometry or spectroscopy and are unable to differentiate between the different models; and similarly the different models themselves do not necessarily provide exclusive predictions for these observables (Arcavi et al. 2017). In addition, as found by De Cia et al. (2018), the specific interpretations of the light curve depend on when during the light curve evolution one is observing.

For the observations of Type Ia and core-collapse SNe, polarimetry has been used as a probe of the three-dimensional structures of these explosions (for a review see Wang & Wheeler 2008). The application of polarimetry may therefore shed light on the possible energy injection mechanism for SLSNe, by being sensitive to

* E-mail: j.maund@sheffield.ac.uk

† y Royal Society Research Fellow

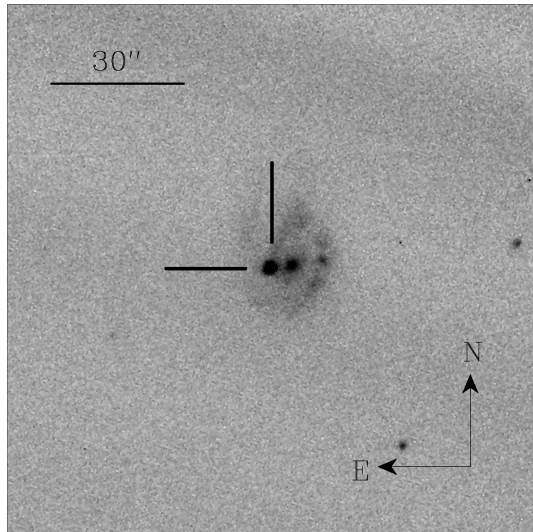


Figure 1. A portion of the LT *RINGO3* ‘green’ image of SN 2017egm (indicated by the cross-hairs) in NGC 3191 on 2017 June 24. The total field size, corresponding to the diameter of the 50 per cent vignettted image, is 246 arcsec.

the geometry of the ejecta (and the underlying sources of excitation) and the processes by which light propagates through the ejecta.

Here we present multicolour polarimetric observations of the superluminous Type I SN 2017egm in the galaxy NGC 3191 (see Fig. 1), acquired with the Liverpool Telescope (LT) *RINGO3* instrument. SN 2017egm was discovered by *Gaia*, as *Gaia* 17biu, on 2017 May 23 (Delgado et al. 2017). With a redshift of $z = 0.03$ for the host galaxy,¹ SN 2017egm is the nearest hydrogen-poor Type I SLSN yet discovered, occurring in a large spiral galaxy in close proximity to the nucleus (see Fig. 1). A number of studies, such as Nicholl et al. (2017) and Wheeler et al. (2017) have presented contradictory interpretations of photometric and spectroscopic observations of this event.

2 OBSERVATIONS AND DATA REDUCTION

SN 2017egm was observed using the Liverpool Telescope (LT) located on the Canary Island of La Palma, using the *RINGO3* polarimeter² (Arnold et al. 2012). Observations were conducted at four separate epochs: 2017 June 24.9, 2017 June 27.9, 2017 July 05.9, 2017 July 08.9 (all dates are UT). These epochs approximately correspond to 4–19 d after the *g*-band light curve maximum (Bose et al. 2018).

Each set of observations of SN 2017egm consisted of 8×74.5 s exposures. *RINGO3* uses a rapidly spinning polaroid to make eight separate measurements of the polarization components of the target source every ~ 2.5 s. A system of two dichroics is used to redirect the light to three separate channels, each with its own camera, covering blue (‘e’ – 3500–6400 Å), green (‘f’ – 6500–7600 Å), and red (‘d’ – 7700–10000 Å) wavelengths each. The bandpasses for the three constituent channels of the *RINGO3* observations and the features

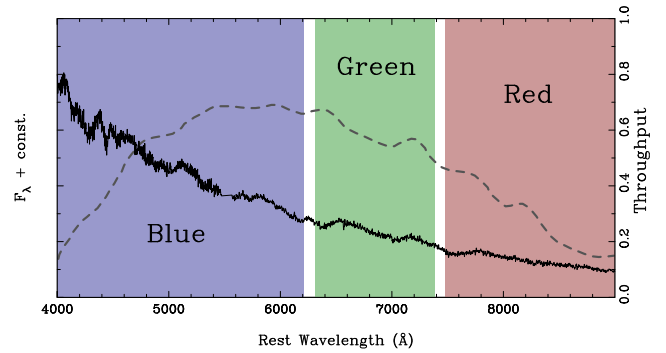


Figure 2. The spectrum of SN 2017egm at +9.1 d post-maximum (Bose et al. 2018) roughly corresponding to the time period covered by our *RINGO3* polarimetric observations. Overlaid are the wavelength regions corresponding to the three *RINGO3* channels and (dashed grey line) the instrumental throughput of *RINGO3* (Arnold 2017).

in the spectrum of SN 2017egm they cover, at these epochs, are shown in Fig. 2.

The *RINGO3* observations were bias and flat-field corrected as part of the instrument data reduction pipeline. Photometry of the sources in the field was conducted using SEXTRACTOR (Bertin & Arnouts 1996), utilizing an aperture of 5 px in diameter uniformly across all images and channels at all polaroid position angles. The sky contribution across the aperture was derived from the background map automatically generated by SEXTRACTOR. The initial calculation of the intensity normalized Stokes $q(= Q/I)$ and $u(= U/I)$ parameters was determined from this photometry following the methodology of Clarke & Neumayer (2002). To calibrate for the effects of polarization induced by the *RINGO3* instrument we followed prescription of Słowikowska et al. (2016). Observations of 324 zero and highly polarized standards, observed between 2017 May 31 and July 31, were used to calibrate for the level of instrumental polarization (q_0 and u_0), the zero angle offset for the polarization angle and the degree of instrumental depolarization, using reference values found in Schmidt, Elston & Lupie (1992) and Hough et al. (2007). In the case of the polarized standards, a low order polynomial was used to convert between the degree and angle of polarization reported in the standard Johnson–Cousins filter system to the wavelength ranges appropriate for the three *RINGO3* channels. The average zero angle offset (K) and the inverse degree of instrumental depolarization (where $D = \text{‘expected polarization’}/\text{‘measured polarization’}$) for each channel, calculated over the long baseline of observations of standards, are presented in Table 1. Our measurements are consistent with previous values determined from zero and polarized standards over longer baselines presented by Jermak (2017) and Arnold (2017). Uncertainties on the observed Stokes parameters were derived using Monte Carlo techniques.

3 RESULTS

The measured polarization properties of SN 2017egm are presented in Table 2 and shown on the Stokes $q - u$ plane in Fig. 3. The evolution of the degree of polarization, with respect to the evolution of the *V*-band photometric light curve is shown in Fig. 4. For individual epochs there is no clear significant level of polarization, with the uncertainty dominated by the systematics associated with the determination of the instrumental depolarization. There are substantially better levels of signal to noise associated with the blue

¹Quoted from the NASA/IPAC Extragalactic Data base - <https://ned.ipac.caltech.edu/>

²<http://telescope.livjm.ac.uk/TelInst/Inst/RINGO3/>

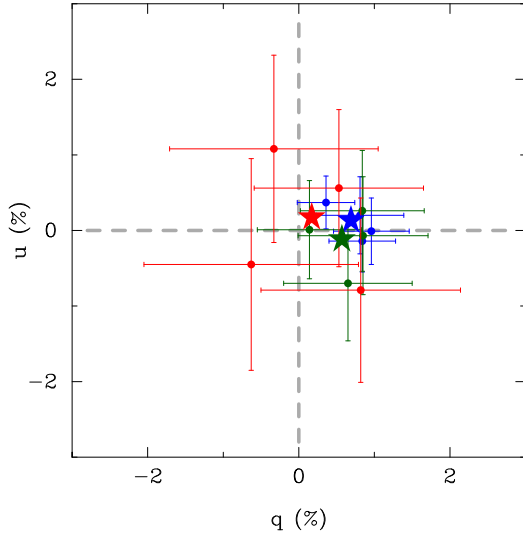
Table 1. Derived instrumental calibration parameters for *RINGO3*.

Detector	q_0 (per cent)	u_0 (per cent)	K ($^\circ$)	D
Blue ('e')	-0.377 ± 0.009	-1.706 ± 0.008	125.2 ± 0.3	1.05 ± 0.02
Green ('f')	-0.910 ± 0.015	-3.239 ± 0.014	125.6 ± 3.2	1.04 ± 0.01
Red ('d')	-1.146 ± 0.022	-3.265 ± 0.020	125.3 ± 0.4	1.02 ± 0.02

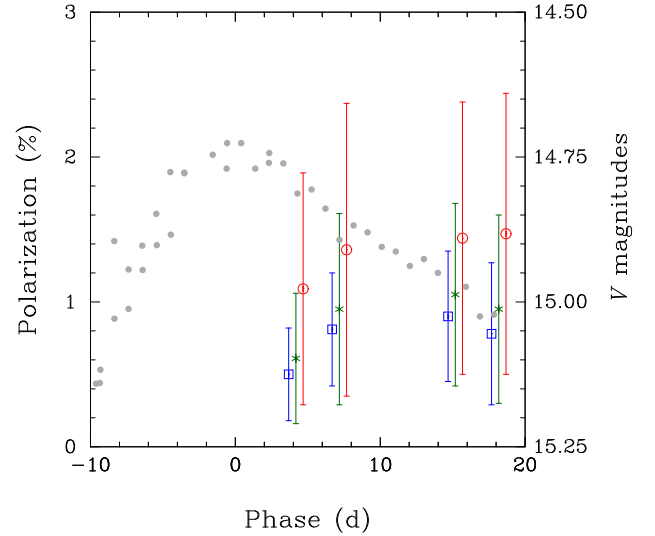
Table 2. Polarimetry of SN 2017egm.

Date (MJD)	Detector	q (per cent)	u (per cent)	p (per cent)	θ ($^\circ$)	V (mag) ^a
2017 Jun 24 (57928.9)	Blue	0.36(0.38)	0.37(0.35)	0.50(0.32)	22.8(26.0)	14.76
	Green	0.14(0.69)	0.01(0.65)	0.61(0.45)	14.0(49.3)	
	Red	0.53(1.12)	0.56(1.04)	1.09(0.80)	21.9(39.0)	
2017 Jun 27 (57931.9)	Blue	0.84(0.44)	-0.14(0.41)	0.81(0.39)	-5.3(17.6)	14.82
	Green	0.84(0.82)	0.26(0.80)	0.95(0.66)	9.9(32.1)	
	Red	-0.63(1.42)	-0.45(1.40)	1.36(1.01)	24.8(62.4)	
2017 Jul 5 (57939.9)	Blue	0.96(0.50)	-0.01(0.44)	0.90(0.45)	-1.1(17.4)	14.94
	Green	0.65(0.85)	-0.70(0.76)	1.05(0.63)	-18.0(31.8)	
	Red	0.82(1.32)	-0.79(1.22)	1.44(0.94)	-11.6(38.4)	
2017 Jul 8 (57942.9)	Blue	0.81(0.58)	0.20(0.51)	0.78(0.49)	6.8(24.7)	15.00
	Green	0.85(0.86)	-0.07(0.78)	0.95(0.65)	-0.2(33.0)	
	Red	-0.33(1.38)	1.08(1.24)	1.47(0.97)	41.9(39.4)	

^aInterpolated V-band magnitude, at the epochs of the *RINGO3* observations, derived from the light curve presented by Bose et al. (2018).

**Figure 3.** The Stokes parameters for SN 2017egm at four separate epochs as presented in Table 2 (●). The points are colour-coded according to the wavelength range of the three *RINGO3* channels. The average Stokes parameters for each wavelength range, reported in Table 3, are presented by the starred points (★).

and green channels, reflecting the blue colour of SN 2017egm at these times (see Fig. 2) and the better sensitivity in these channels. In Table 3 we present the weighted-average polarization derived across all four epochs and find some possible evidence for marginal polarization at blue wavelengths, with the highest levels of signal to noise, which may indicate that any polarization signal, if present, is preferentially associated with the Stokes q parameter.

**Figure 4.** The evolution of the degree of polarization of SN 2017egm with time. The points indicate the polarization measured through the ‘blue’ (□), ‘green’ (*), and ‘red’ (○) *RINGO3* channels. Also shown, in grey, is the V-band light curve reported by Bose et al. (2018).**Table 3.** Average polarimetric properties of SN 2017egm.

Detector	q (per cent)	u (per cent)	p (per cent)	θ ($^\circ$)
Blue	0.69(0.23)	0.13(0.21)	0.63(0.23)	5.3(14.5)
Green	0.57(0.40)	-0.12(0.37)	0.31(0.40)	-6.0(34.0)
Red	0.17(0.65)	0.17(0.60)	0.24(0.63)	22.5(180)

Following the spectral evolution of SN 2017egm reported by Bose et al. (2018), the intrinsic polarization in the three *RINGO3* bandpasses are expected to be dominated by wavelength-independent continuum polarization, with possible contamination from polarization that might be associated with lines of Fe II in the blue bandpass, Si II in the green bandpass and O I and Ca II in the red bandpass.

The data have not been corrected for the interstellar polarization (ISP) which, for broad-band imaging polarimetry, is generally difficult to determine for the full dust column to the target SN (including the host galaxy contribution). SN 2017egm, and its host galaxy, are located opposite the Galactic centre and at a relatively high Galactic latitude ($b = 54^\circ$), with the Galactic extinction in the direction of the SN corresponding to $E(B - V) = 0.0097 \pm 0.0005$ mag (Schlafly & Finkbeiner 2011), implying the ISP arising in the Galaxy is likely to be low (given $p_{\text{ISP}} < 9 \times E(B - V)$ per cent assuming a Serkowski, Mathewson & Ford 1975 polarization correlation, such that for SN 2017egm $p_{\text{ISP}} < 0.09$ per cent). This expectation is confirmed by HD 89021 (located $\sim 3.56^\circ$ from the SN line of sight) in the Heiles (2000) catalogue, for which the measured polarization is only $p = 0.010 \pm 0.120$ per cent. If we are to believe the slight preference for polarization signal, in the blue and green channels, being found in the Stokes q parameter, i.e. $\theta \rightarrow 0^\circ$, this might be consistent with the apparent orientation of the spiral arm containing SN 2017egm in the galaxy NGC 3191 appearing to lie approximately North–South, with the SN located almost due East of the host galaxy nucleus (see Fig. 1). Given the expectation that the ISP arising from dust grains in other galaxies should run parallel to the magnetic field lines running along spiral arms (Scarrott, Ward-Thompson & Warren-Smith 1987), the slight preference for positive Stokes q may reflect an ISP contribution arising in spiral arm of NGC 3191 and the observed polarization is not intrinsic to SN 2017egm itself.

4 DISCUSSION & CONCLUSIONS

The lack of a significant detection of polarization, at individual epochs, associated with SN 2017egm is consistent with the generally low levels of polarization previously measured for other Type I SLSNe. The polarization levels measured here are consistent with the limited spectropolarimetry reported by Bose et al. (2018) at comparable epochs from -1 to $+9$ d. Bose et al. claim a significant detection at the level of $p \sim 0.43 \pm 0.09$ per cent with a polarization angle of $-19 \pm 6^\circ$ over a wavelength range approximately corresponding to our ‘red’ observation. These levels are consistent with the average polarization and polarization angle measured from our *RINGO3* observations, and confirm the preference for the polarization signal to occur in Stokes q . Although Bose et al. (2018) claim that the lack of strong wavelength dependence to the polarization is inconsistent with a Serkowski et al. (1975) ISP law, it is important to remember that at low polarization levels the wavelength dependence may be difficult to discern (see e.g. Reilly et al. 2016) to the point of irrelevance and this situation may be especially compounded in instances of low signal to noise. Although Bose et al. (2018) do identify possible evidence for modulation of the polarization across spectral features, some of these regions are associated with strong sky absorption and emission features (and may not be not intrinsic to the SN).

Our polarization measurements of SN 2017egm, associated with maximum light, are consistent with an almost spherical photosphere. Our limits on the degree of polarization, for no ISP, constrain departures from a spherical symmetry, assuming an underly-

ing oblate spheroidal structure, to an axial ratio of >0.85 (Höflich 1991). Indeed, the observation of suppression of flux at ultraviolet wavelengths, due to significant line opacity (Yan et al. 2018), may imply that the bluer wavelengths of our data, down to the atmospheric cut-off, could be intrinsically depolarized (similar to Type Ia SNe; see e.g. Maund et al. 2013), and therefore this wavelength region is most likely representative of the ISP. Unless there were some fortuitous anti-alignment of the ISP and intrinsic polarization of the SN, our limited evidence would support an axial ratio for the SN that is close to unity.

The low levels of polarization are consistent with previously reported polarimetry of the Type I SLSNe LSQ14mo (Leloudas et al. 2015, 2017b) and SN 2015bn (Inserra et al. 2016; Leloudas et al. 2017a). For LSQ14mo, Leloudas et al. (2015) observed similar levels of polarization, in imaging polarimetry at five epochs spanning -7 to $+19$ d relative to the light curve maximum. Leloudas et al. inferred an almost spherical ejecta with limits on the axial ratio for an ellipsoidal configuration of >0.9 . The combined observations of SN 2015bn presented by Inserra et al. (2016) and Leloudas et al. (2017a) covered a large time range of -24 to $+27$ d and -20 to $+40$ d, relative to the light curve maximum, respectively. From these observations, including two epochs of spectropolarimetry, a more complex picture of the evolution of the polarization of SLSNe emerged. Both Inserra et al. and Leloudas et al. observed a fundamental change in the polarization properties of that SN, consistent with ejecta becoming more asymmetric with depth. Such ‘phase transitions’ might not be unexpected, and certainly the presence of discontinuities in the geometries of the ejecta of normal SNe have been previously witnessed through polarimetry (Leonard et al. 2006; Maund et al. 2009). As noted by De Cia et al. (2018), significant quantities of Ni ($1-10 M_\odot$) are required to power the late-time light curves of Type I SLSNe. Unless there are significant asymmetries (inconsistent with polarimetric measurements) an alternative mechanism must be responsible for the luminosity around the light curve maximum. It is conceivable that if a more extended baseline of observations of SN2017egm were available a similar change in the polarization characteristics of the SN might have been observed. In addition, Inserra et al. observed a wavelength dependence in the degree of polarization across the spectrum of SN 2015bn at the two epochs. They claimed this could be due to an internal engine such as a magnetar or could be due to the wavelength dependence of the significant opacity due to large quantities of metals in the ejecta (possibly indicating a pair-instability event). Such rises in polarization at redder wavelengths, due to a relative decrease in line opacity, have been previously seen in Type Ia SNe (Howell et al. 2001; Patat et al. 2012). Unfortunately, given the range of signal to noise in our observations in the different *RINGO3* channels, it is not possible to discern if there is any wavelength dependence.

A note of caution is, however, required in the comparison between the polarimetric properties of SN 2017egm and those of other Type I SLSNe. It has been remarked that both the location, with respect to the host galaxy, and the photometric evolution of SN 2017egm are peculiar. Chen et al. (2017) determined the metallicity at the region of the SN in NGC 3191, finding solar or just above solar abundances (alternatively, Izzo et al. 2018 derive lower metallicities and estimate an initial progenitor mass $>20 M_\odot$). Wheeler et al. (2017) observed that the shape of the peak of the light curve was unlike those of magnetar-powered models, instead being consistent with collision of the ejecta with a dense shell of circumstellar material (CSM). Unlike spectropolarimetry of the interacting, possible impostor SN 2009ip (Mauerhan et al. 2014; Reilly et al. 2017),

the lack of strong polarization for SN 2017egm may imply that the CSM completely encloses the ejecta, providing a spherical contact surface that maximizes the efficiency of the conversion of kinetic energy of the ejecta to radiative energy. If the light curve peaks of Type I SLSNe are generally produced by CSM interaction, the published polarimetry of these objects all suggest spherical symmetry is a key ingredient.

From our observations we can exclude significant levels of polarization for SN 2017egm, around maximum light, that is commonly associated with core-collapse SNe. The precision of our polarization measurements are limited by a small, but non-negligible degree of polarization arising from *RINGO3*. Future designs for a high time resolution polarimeter with the Liverpool Telescope Multiwavelength OPTimized Optical Polarimeter (MOPTOP; Jermak, Steele & Smith 2016, 2017) will use a dual-beam design, with throughput increased by a factor of ~ 2 compared to *RINGO3*, and will yield polarization precisions < 0.1 per cent. MOPTOP will provide a unique and powerful observing mode on a two-metre telescope for efficient polarimetric follow-up of transients in the next decade.

ACKNOWLEDGEMENTS

The research of JRM is supported through a Royal Society University Research Fellowship. The research of JCW is supported in part by the Samuel T. and Fern Yanagisawa Regents Professorship in Astronomy.

The Liverpool Telescope is operated on the island of La Palma by Liverpool John Moores University in the Spanish Observatorio del Roque de los Muchachos of the Instituto de Astrofísica de Canarias with financial support from the UK Science and Technology Facilities Council.

REFERENCES

- Arcavi I. et al., 2017, *Nature*, 551, 210
- Arnold D., 2017, PhD thesis, Astrophysics Research Institute, Liverpool John Moores University
- Arnold D. M., Steele I. A., Bates S. D., Mottram C. J., Smith R. J., 2012, in McLean I. S., Ramsay S. K., Takami H., eds, Proc. SPIE Conf. Ser. Vol. 8446, Ground-based and Airborne Instrumentation for Astronomy IV. SPIE, Bellingham, p. 84462J
- Bertin E., Arnouts S., 1996, *A&AS*, 117, 393
- Bose S. et al., 2018, *ApJ*, 853, 57
- Chatzopoulos E., Wheeler J. C., 2012, *ApJ*, 760, 154
- Chen T.-W. et al., 2017, *ApJ*, 849, L4
- Clarke D., Neumayer D., 2002, *A&A*, 383, 360
- De Cia A. et al., 2018, *ApJ*, 860, 100
- Delgado A., Harrison D., Hodgkin S., Leeuwen M. V., Rixon G., Yoldas A., 2017, Transient Name Server Discovery Report, 591
- Dong S. et al., 2016, *Science*, 351, 257
- Gal-Yam A., 2012, *Science*, 337, 927
- Gal-Yam A. et al., 2009, *Nature*, 462, 624
- Heiles C., 2000, *AJ*, 119, 923
- Höflich P., 1991, *A&A*, 246, 481
- Hough J. H., Lucas P. W., Bailey J. A., Tamura M., 2007, in Sterken C., ed., ASP Conf. Ser. Vol. 364, The Future of Photometric, Spectrophotometric and Polarimetric Standardization. Astron. Soc. Pac., San Francisco, p. 523
- Howell D. A., Höflich P., Wang L., Wheeler J. C., 2001, *ApJ*, 556, 302
- Insera C., Bulla M., Sim S. A., Smartt S. J., 2016, *ApJ*, 831, 79
- Izzo L. et al., 2018, *A&A*, 610, A11
- Jermak H., 2017, PhD thesis, Astrophysics Research Institute, Liverpool John Moores University
- Jermak H., Steele I. A., Smith R. J., 2016, in Evans C. J., Simard L., Takami H., eds, Proc. SPIE Conf. Ser. Vol. 9908, Ground-based and Airborne Instrumentation for Astronomy VI. SPIE, Bellingham, p. 99084I
- Jermak H., Steele I. A., Smith R. J., 2017, in Gomboc A., ed., Proc. IAU Symp. 324, New Frontiers in Black Hole Astrophysics. Kluwer, Dordrecht, p. 357
- Kasen D., Bildsten L., 2010, *ApJ*, 717, 245
- Leloudas G. et al., 2015, *ApJ*, 815, L10
- Leloudas G. et al., 2016, *Nature Astron.*, 1, 0002
- Leloudas G. et al., 2017a, *ApJ*, 837, L14
- Leloudas G. et al., 2017b, *ApJ*, 843, L17
- Leonard D. C. et al., 2006, *Nature*, 440, 505
- Mauerhan J. et al., 2014, *MNRAS*, 442, 1166
- Maund J. R., Wheeler J. C., Baade D., Patat F., Höflich P., Wang L., Clocchiatti A., 2009, *ApJ*, 705, 1139
- Maund J. R. et al., 2013, *MNRAS*, 433, L20
- Nicholl M., Berger E., Margutti R., Blanchard P. K., Guillochon J., Leja J., Chornock R., 2017, *ApJ*, 845, L8
- Patat F., Höflich P., Baade D., Maund J. R., Wang L., Wheeler J. C., 2012, *A&A*, 545, A7
- Quimby R. M., Aldering G., Wheeler J. C., Höflich P., Akerlof C. W., Rykoff E. S., 2007, *ApJ*, 668, L99
- Reilly E. et al., 2016, *MNRAS*, 457, 288
- Reilly E., Maund J. R., Baade D., Wheeler J. C., Höflich P., Spyromilio J., Patat F., Wang L., 2017, *MNRAS*, 470, 1491
- Scarrott S. M., Ward-Thompson D., Warren-Smith R. F., 1987, *MNRAS*, 224, 299
- Schlafly E. F., Finkbeiner D. P., 2011, *ApJ*, 737, 103
- Schmidt G. D., Elston R., Lupie O. L., 1992, *AJ*, 104, 1563
- Serkowski K., Mathewson D. L., Ford V. L., 1975, *ApJ*, 196, 261
- Śłowikowska A., Krzeszowski K., Żejmo M., Reig P., Steele I., 2016, *MNRAS*, 458, 759
- Smith N. et al., 2007, *ApJ*, 666, 1116
- Wang L., Wheeler J. C., 2008, *ARA&A*, 46, 433
- Wheeler J. C., Chatzopoulos E., Vinkó J., Tuminello R., 2017, *ApJ*, 851, L14
- Woosley S. E., Blinnikov S., Heger A., 2007, *Nature*, 450, 390
- Yan L., Perley D. A., De Cia A., Quimby R., Lunnan R., Rubin K. H. R., Brown P. J., 2018, *ApJ*, 858, 91

This paper has been typeset from a \LaTeX file prepared by the author.